Nuclear Physics **A458** (1986) 637-651
North-Holland, Amsterdam

RADIATIVE CAPTURE OF POLARIZED NEUTRONS BY HYDROGEN BELOW THE PION PRODUCTION THRESHOLD

J.M. CAMERON, C.A. DAVIS, H. FIELDING, P. KITCHING, J. PASOS, J. SOUKUP, J. UEGAKI, J. WESICK and H.S. WILSON

University of Alberta, Edmonton, Alberta, Canada T6G 2J1

R. ABEGG, D.A. HUTCHEON and C.A. MILLER

TRIUMF, 4004 Wesbrook Mall, Vancouver, BC, Canada V6T 2A3

A.W. STETZ

Oregon State University, Corvallis, Oregon 97331 USA

I.J. VAN HEERDEN

University of the Western Cape, Private Bag X17, Belleville 7530, Republic of South Africa

Received 12 May 1986

Abstract: We report the results of measurements of the differential cross section and analyzing power for the radiative capture of polarized neutrons by hydrogen at $E_n = 180$ and 270 MeV. The experimental results are compared to predictions of various theoretical models of this process to examine the sensitivity to details of the short range part of the NN interaction and to those contributions which arise due to non-nucleonic degrees of freedom in the interaction of the photon with the nucleus.

E | NUCLEAR REACTIONS ^{1}H (polarized n, γ), $E = 180$, 270 MeV; measured $\sigma(\theta)$, $A(\theta)$.

1. Introduction

Interest in the study of radiative capture to, or photodisintegration of, the deuteron has undergone a recent renaissance. This renewed attention is one consequence of attempts to understand the role of non-nucleonic degrees of freedom in nuclei. Here the use of photons as a nuclear probe, where the primary interaction is well understood, has clear advantages. The photon coupling to the nucleons which dominates at low momentum transfer is known to be largely insufficient already at $E_\gamma = 100$ MeV and one has a clear demonstration of the importance of meson exchange currents (MEC) wherein the photon coupled to the pions which mediate the NN interaction.

Many calculations, however, suffer from a lack of consistency [1]), for example in not using the same NN potential to calculate the wave functions and to derive the exchange current operators. There are also problems with different reference frames

being used for the initial state, operators, and final states. This neglect will have important consequences in any comparison between theory and experiment [2]). The importance of relativistic corrections to the charge and current operators has been highlighted by attempts to understand the zero degree differential cross section data [3]) which differed substantially from the predictions of a nonrelativistic impulse approximation calculation [4]). This discrepancy appears mainly to arise from the neglect of the relativistic spin orbit correction term [5-7]).

The deficiencies in many of the models of photodisintegration would no doubt have been evident sooner had reliable experimental data been available. This, however, was not the case as is demonstrated in fig. 1 where experimental data at $E_\gamma = 95$ MeV, which were published prior to 1985 are shown [3,8-13]). Most experiments were performed using bremsstrahlung photon beams and liquid deuterium targets and it is clear that many did not obtain the correct normalization. This situation is now being rectified by new information obtained using tagged photon beams or neutron radiative capture [14]).

Evidently differential cross section data alone will not be sufficient to separate contributions from the several effects discussed above. To this end we have for the first time in this energy range measured in addition the asymmetry obtained using

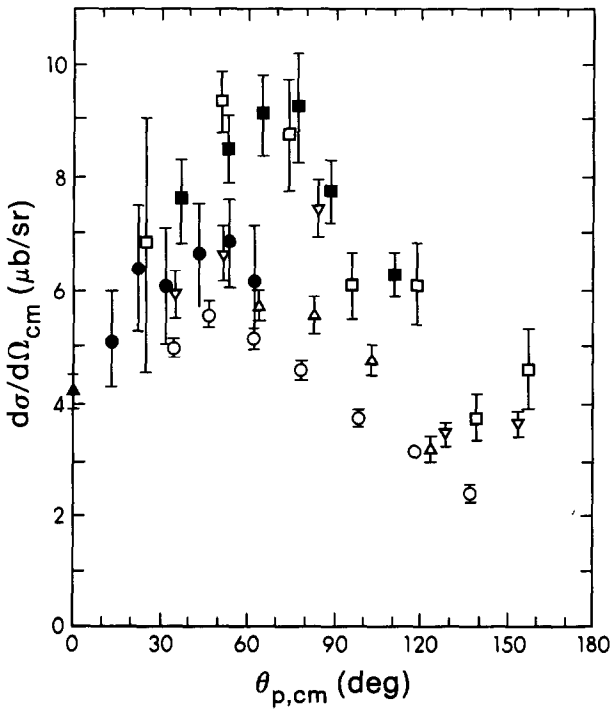

Fig. 1. Data for deuteron photodisintegration available prior to 1984. The data are from ref. [3]) (△); ref. [8]) (▽); ref. [10]) (□); ref. [11]) (○); ref. [12]) (■) and ref. [13]) (●).

polarized neutrons. In this paper we present details of our measurements of the differential cross section and asymmetry for neutron energies of $E_n = 180$ and 270 MeV. These data are compared with the predictions of several representative model calculations.

2. Experimental method

The experiment was performed using the TRIUMF neutron beam facility [15]) in which polarized neutrons are produced via the large transverse polarization transfer, r_t, in the $^2H(\vec{p}, \vec{n})2p$ reaction at 9° lab using a 20 cm long liquid deuterium target. The transverse polarized proton beam is obtained using a superconducting precession solenoid to rotate the proton spin by 90° into the horizontal plane. Neutrons at the reaction angle of 9° pass through a 3.37 m lead collimator and through two dipole magnets which precess the transverse component of neutron polarization into the vertical. They also serve to remove unwanted charged particles from the beam. The calibration of all three spin precession magnets was carried out by measuring the left-right and up-down asymmetries in a neutron polarimeter. This latter consisted of a polyethylene target and four identical scintillator counters at nominal scattering angles of $\theta = 30°$ and $\phi = 0$, 90, 180, 270° which detected protons ejected from the target. The neutron beam profile was also measured frequently using a scintillator convertor and two delay line wire chambers to give X and Y coordinates. This device was positioned 4.32 m downstream of the primary experiment target location. The size of the neutron beam at the latter position was 9 cm FWHM vertically. With a typical proton beam of 250 nA and 70% polarization the neutron beam had an intensity of 1.5×10^6 s^{-1} and polarization of about 60%.

The proton beam intensity and average polarization for the three ion source conditions giving spin up, down, and off were determined using a polarimeter in the beamline upstream of the LD_2 target as described in ref. [15]).

The liquid hydrogen flask and vacuum vessel were designed to minimize the material in the horizontal scattering plane. The target cells used were 11 cm in diameter and the thicknesses were chosen to give a hydrogen thickness of 0.3 g/cm^2 for 180 MeV and 0.7 g/cm^2 for 270 MeV runs. For target empty measurements the liquid hydrogen in the cell could be replaced by cold hydrogen gas.

The detection system, shown schematically in fig. 2, was left-right symmetric with each half consisting of a deuteron detector in coincidence with four γ-ray detectors. The γ-rays were detected in lead-glass Cherenkov detectors placed at distances from the target of 0.55 to 1.3 m depending on angle. Each deuteron detector consisted of a 10 cm thick by 30 cm wide by 35 cm tall plastic scintillator followed by a veto scintillator to allow rejection of passing protons from the np→pn reaction. Two delay line readout multiwire chambers allowing determination of deuteron trajectories. The wire chamber data were only used to confirm that the deuteron counters were large enough to intercept all coincident deuterons despite effects of finite

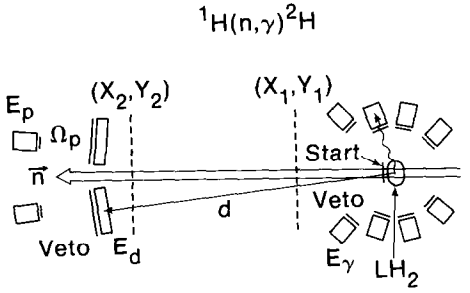

Fig. 2. Schematic diagram of the experimental set-up.

neutron beam size, γ-ray acceptance, and deuteron multiple scattering. The angular acceptance and resolution was, however, determined by the sizes of the γ counters, the target, and beam. A 1.5 mm thick plastic scintillator (start) was placed directly behind the target and covered the total cone of ejected deuterons while a similar detector placed just before the target was used to reject any events initiated by charged particles in the beam.

The counters denoted as Ω_p and E_p were used to detect recoil protons at an angle of 6° (lab) and were respectively small plastic scintillators which defined the solid angle and 12.5 cm diameter × 12.5 cm thick NaI crystals.

A fast coincidence between a Cherenkov and a deuteron counter was used to select events which were processed through a CAMAC data link to be recorded on magnetic tape. A trigger based on a prescaled sample of the $\Omega_p E_p$ coincidence events operated independently and selected elastic scattering events which were similarly recorded. For each coincidence event the pulse heights in all detectors, the time difference between the various pulses and that from the start counter, and the x and y coordinates of both wire chambers were recorded. In addition, a digital register recorded information on the polarization state and the type of event (singles, coincidence, or pulser). Approximately 10% of events recorded were generated by feeding a randomly triggered pulser signal to all detectors. The trigger was determined using a signal from one of the proton polarimeter detectors and thus had a rate proportional to the beam current.

Events recorded on magnetic tape were analyzed off-line in a number of stages. First, all coincidence events were separated from others and analyzed independently. Next, cuts were made on $E-T$ and $E-\Delta E$ to select deuterons; a typical $E-T$ plot is shown in fig. 3. A cut was then applied to the time difference between Cherenkov and start signals to select real coincidence events and an identical window in time, displaced by one cyclotron beam burst (43 nsec), was used to determine the accidental coincidence rate. Events which were initiated by low-energy neutrons produced in the deuterium production target were excluded by putting a cut on the time difference between the start counter and the cyclotron RF signal; the main neutron beam which remains has a FWHM of about 17 MeV at $E_n = 180$ MeV and

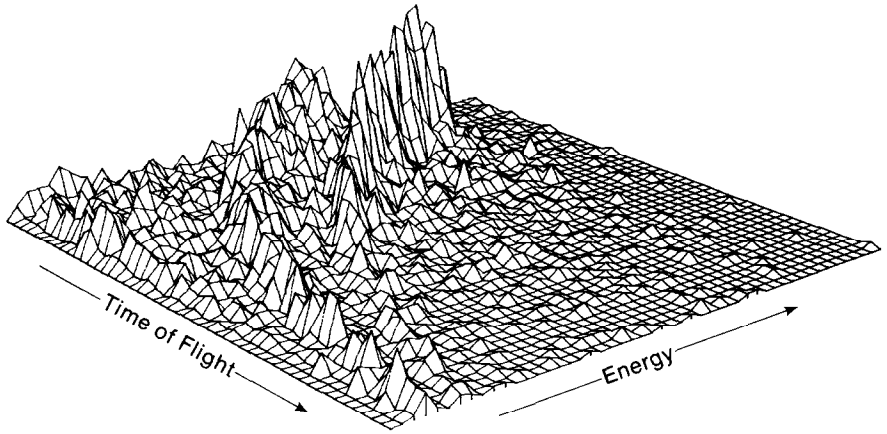

Fig. 3. Isometric display of time-of-flight versus energy for charged particles. The two loci correspond to protons and deuterons. The target empty background has not been subtracted in the figure.

13 MeV at $E_n = 270$ MeV. Finally an energy cut was applied to the deuteron pulse height. Events were then separated according to the polarization of the incident proton beam.

Proton events corresponding to back-angle elastic scattering were also subject to time of flight cuts, the same criteria being applied to the neutron time of flight spectra as was done for the $d-\gamma$ coincidence events.

Losses of protons and deuterons due to scattering and reactions have been calculated from the available cross section data. A check of these estimates has been made at the laboratoire National Saturne by directing a low intensity 190 MeV deuteron beam into one of the plastic detectors; a reaction tail of $(34 \pm 2)\%$ was found in good accord with the estimated losses.

Corrections were also applied for photon detection efficiency of the Cherenkov detectors and for photons absorbed between the target and these detectors. The method used in determining the photon efficiency of the Cherenkov detectors has been described previously [16]).

3. Results

The results of the present experiment are given in table 1. The analyzing power data have been published previously [17]) but are repeated here for completeness. The differential cross sections are normalized to the elastic scattering yield measured at 168° c.m. The values for the latter, taken from the interactive phase shift program SAID [18]), were $\sigma = 9.76$ μb/sr at $E_n = 180$ MeV and $\sigma = 8.05$ μb/sr at $E_n = 270$ MeV. Any change in the accepted value of these np elastic scattering cross sections will impose a renormalization of these radiative capture data.

The errors given in table 1 are only those due to counting statistics. The cross sections are subject to an overall additional scale error of 5.4% arising from

TABLE 1

Experimental results for the differential cross section and analyzing powers for the reaction $\vec{n}p \to d\gamma$ at $E = 180$ and 270 MeV

$E_n = 180$ MeV					$E_n = 270$ MeV				
θ_n	$\sigma(\theta)$	$\Delta\sigma(\theta)$(μb/sr)	A_y	ΔA_y	θ_n	$\sigma(\theta)$	$\Delta\sigma(\theta)$(μb/sr)	A_y	ΔA_y
32.2	0.326	0.017	0.092	0.087	31.5	0.483	0.013	−0.083	0.058
37.4	0.511	0.033	0.092	0.147	34.2	0.537	0.028		
48.8	0.487	0.024	−0.096	0.086	49.1	0.655	0.012	−0.111	0.037
52.6	0.563	0.020	−0.039	0.065	55.6	0.824	0.035		
76.1	0.822	0.036	−0.039	0.066	74.0	0.859	0.016	−0.145	0.049
97.4	0.949	0.038	−0.136	0.056	95.0	0.960	0.018	−0.207	0.039
119.2	0.862	0.032	−0.253	0.059	116.3	0.988	0.019	−0.268	0.043
124.5	1.021	0.026	−0.253	0.050	119.8	0.996	0.039	−0.340	0.068
138.0	0.915	0.044	−0.165	0.172	131.7	0.919	0.027	−0.395	0.070
142.1	0.814	0.030	−0.169	0.060	144.3	0.778	0.022	−0.345	0.055

uncertainty in solid angles (2%) to the evaluation of reaction losses of charged particles in the charged particle detectors (3%) and to the efficiency of the Cherenkov detectors (4%). Furthermore the data are normalized using the values for np elastic scattering cited and uncertainty in this value is not included in the error as renormalization is possible. An estimate of this uncertainty might be taken from comparing the predictions of different phase shift analysis which differ by some 2 to 3% [ref. [18])]. The analyzing power data are also subject to a scale uncertainty due to the value of r_t used in determination of the neutron beam polarization. Again differences between various phase shift solutions for r_t would indicate an uncertainty 1.5% [ref.[18])] while the proton beam polarimeter calibration introduces an additional 2%. The overall scale uncertainty in the measured asymmetries is thus 0.025.

The present cross-section measurements are compared in fig. 4 to other recent data obtained using either neutron radiative capture [19]) or monochromatic photons [20]). These new data sets are seen to be in excellent agreement in contrast to the prior situation as summarized in fig. 1.

4. Comparison with model predictions

In this section we compare the experimental data to predictions of several theoretical models, chosen to be representative of those used recently to describe this process. Using these comparisons we comment on several current concerns: (i) What is the sensitivity to the (unknown) details of the NN interaction at short range as incorporated in different N potentials (ii) What is the role of meson exchange currents and (iii) What is the effect of relativistic corrections to the one- and two-body charge operators?

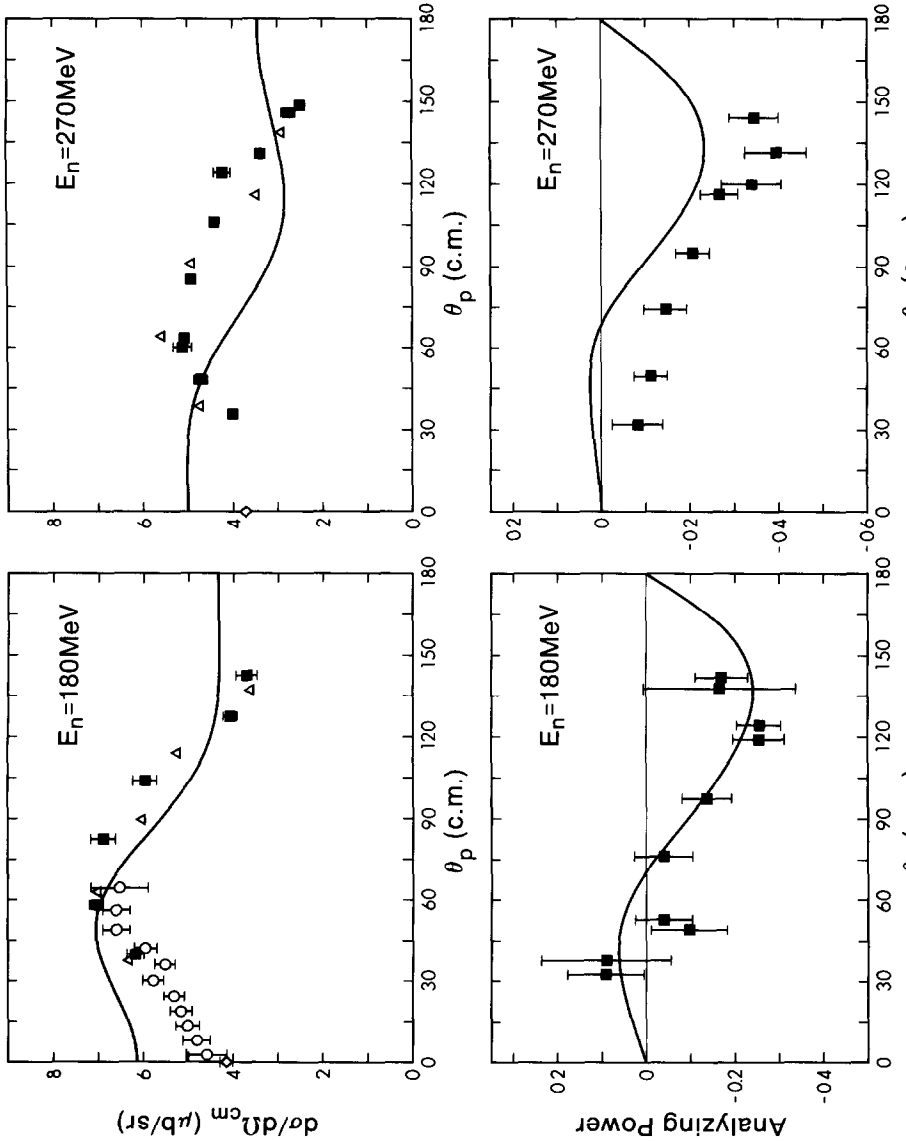

Fig. 4. Results of the present experiment are presented (■) and compared to other recent measurements made using radiative capture ref. [19]) (○) and with monochromatic photons, ref. [20]) (△). The radiative capture cross section data are converted using detailed balance and are plotted as a function of the proton center of mass angle. The zero degree data of ref. [3]) are also shown (◇). The solid curves show Partovi's (ref. [4])) calculation based on the Hamada-Johnston potential (ref. [23])).

The simplest picture of a photo nuclear process is one where the photon is coupled (minimally) to the nucleons. That this basic contribution is insufficient at the energies of our experiment is well known and indeed does not alone satisfy the continuity equation [21]). When the operator is modified to again conserve current, one obtains the form given by Siegert's theorem [22]) wherein meson exchange current contributions to the dominant A1 operator are now implicitly included. These contributions are model independent in that they are determined by the potential being used for the NN force. This is generally taken as the basic calculation for photodisintegration below pion threshold and results are most frequently quoted from the comprehensive work of Partovi [4]) who used the Hamada-Johnston NN potential [23]). The results obtained are shown in fig. 4. It is now apparent that there are major discrepancies in both cross section and analyzing powers. This point has indeed already been made in connection with the zero-degree cross section where the recent accurate data [3]) lie considerably below the predicted values.

As seen in fig. 5 the cross section predicted in the impulse approximation does appear to be sensitive to the NN potential used [24]). Much of this dependence, is however attributable to differences in the D state component of the deuteron wave function and disappears for most potentials when the results are scaled to the known value of the asymptotic S to D state ratio η [ref. [5])]. One exception is the Hamada-Johnston potential used by Partovi, which also gives an incorrect deuteron binding energy [5]).

The situation is seen to be quite different for the analyzing powers where there appears to be little dependence on the details of the NN potentials. This point has been emphasized in calculations using phase equivalent modifications of the short range part of the wavefunctions [25]). It was found that while such modifications cause marked changes in the predicted cross section and photon asymmetry there was little change in the analyzing power.

A one Boson exchange potential now widely used in nuclear physics is the parametrized form of the Paris potential obtained from a dispersion theoretical approach to NN scattering [26]). Recently several calculations of deuteron photodisintegration have been made using this potential and we limit our further discussion to these.

The classical potential model approach may be improved by adding effects due to the coupling of the photon with the exchanged mesons as required by gauge invariance. In ref. [24]) the two-body change density from one pion exchange and two-body current density due to π, ρ and ω meson exchange have been incorporated using pseudovector coupling in an approach otherwise equivalent to that of Partovi [4]). The predictions without (solid curves) and including these two body current (dotted) and also charge effects (dashed lines) are shown in fig. 6. On one hand the effect of both correction terms is to increase the predicted differential cross section which is then higher than experiment at both energies while on the other hand the agreement with the analyzing power data at $E_n = 280$ is much better when

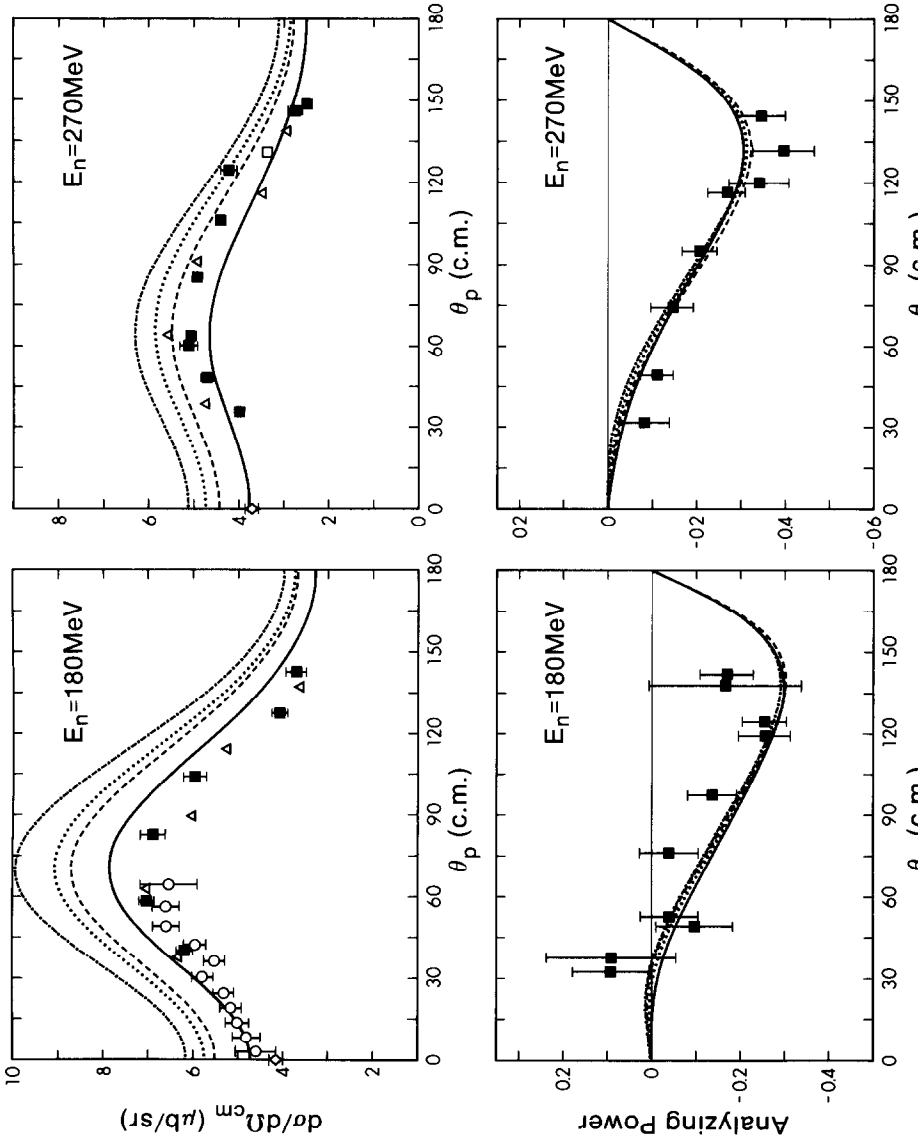

Fig. 5. Recent experimental results, as cited for fig. 4, are compared to calculations (from ref. [24]) which include two body charge and current corrections for four different NN potentials. The solid curve corresponds to the super-soft-core (SSC) of deTourreil and Sprung (ref. [27])), the dashed line to the Paris potential (ref. [26])), the dotted line to the Yale potential (ref. [28])) and the dot-dash line to the Hamada–Johnston potential (ref. [23])).

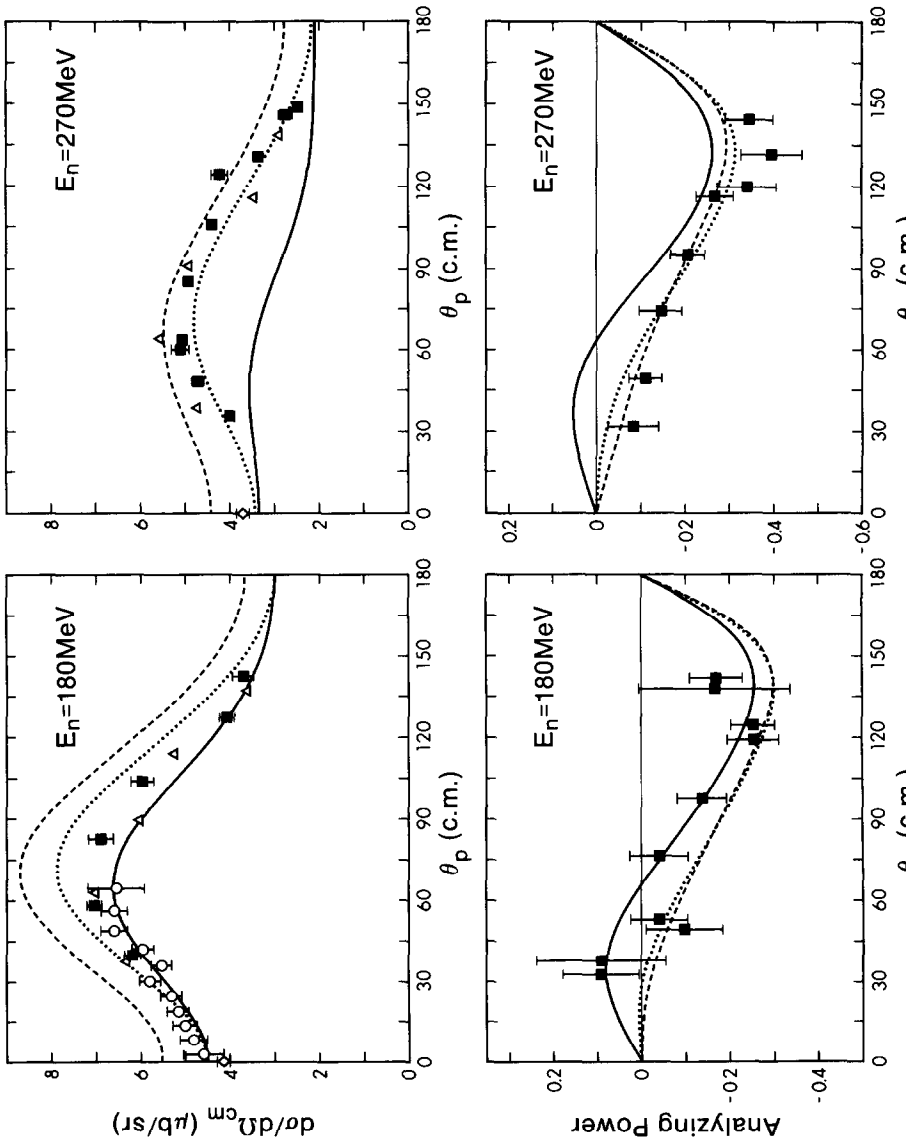

Fig. 6. The recent experimental results, as cited for fig. 4, are compared to calculations (ref. [24])) in which exchange effects are neglected (solid curve), where current density effects owing to π, ρ, and ω exchange are included (dotted curve) and when the charge density effects due to π exchange are added (dashed curve).

the exchange currents are incorporated but the further addition of the charge corrections has little effect.

A further reduction in the calculated cross section is obtained by including relativistic corrections to the one body charge operator [5-7]). The differential cross sections predicted by Cambi *et al.* [6]) are compared to the recent data in fig. 7 and good overall agreement is now seen at both energies. The recent calculations of Jaus and Woolcock [7]) are in good accord with those of Cambi *et al.* The former emphasize the clear preference of the data for pseudovector over pseudoscalar coupling. They also demonstrate that there is considerable improvement when the

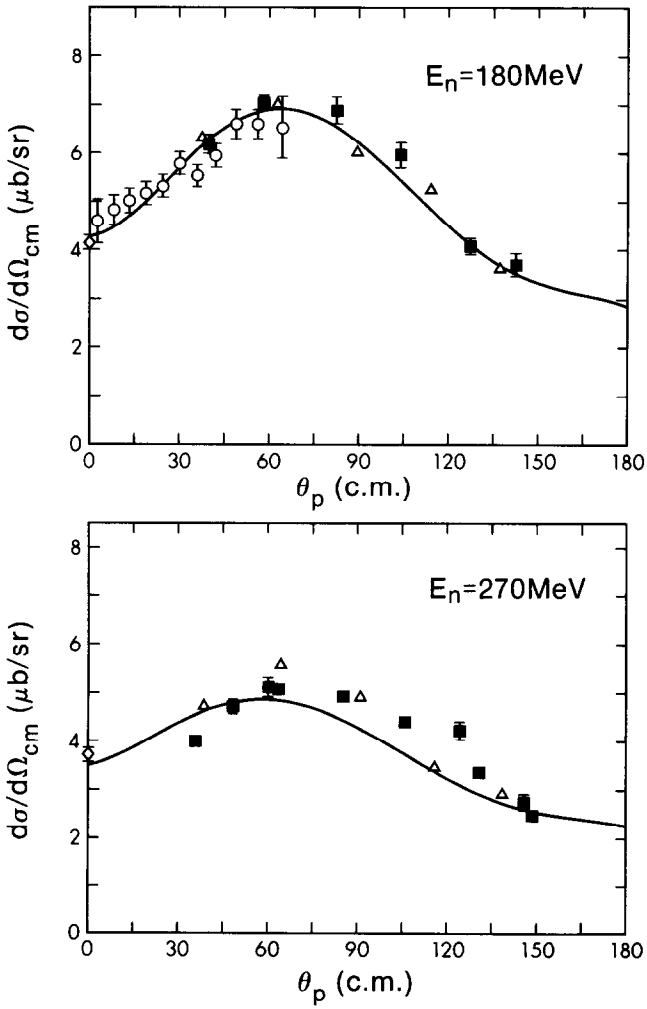

Fig. 7. The recent differential cross section results, as cited for fig. 4, are compared to calculations (ref. [6])) where relativistic corrections to the one-body charge operator are included.

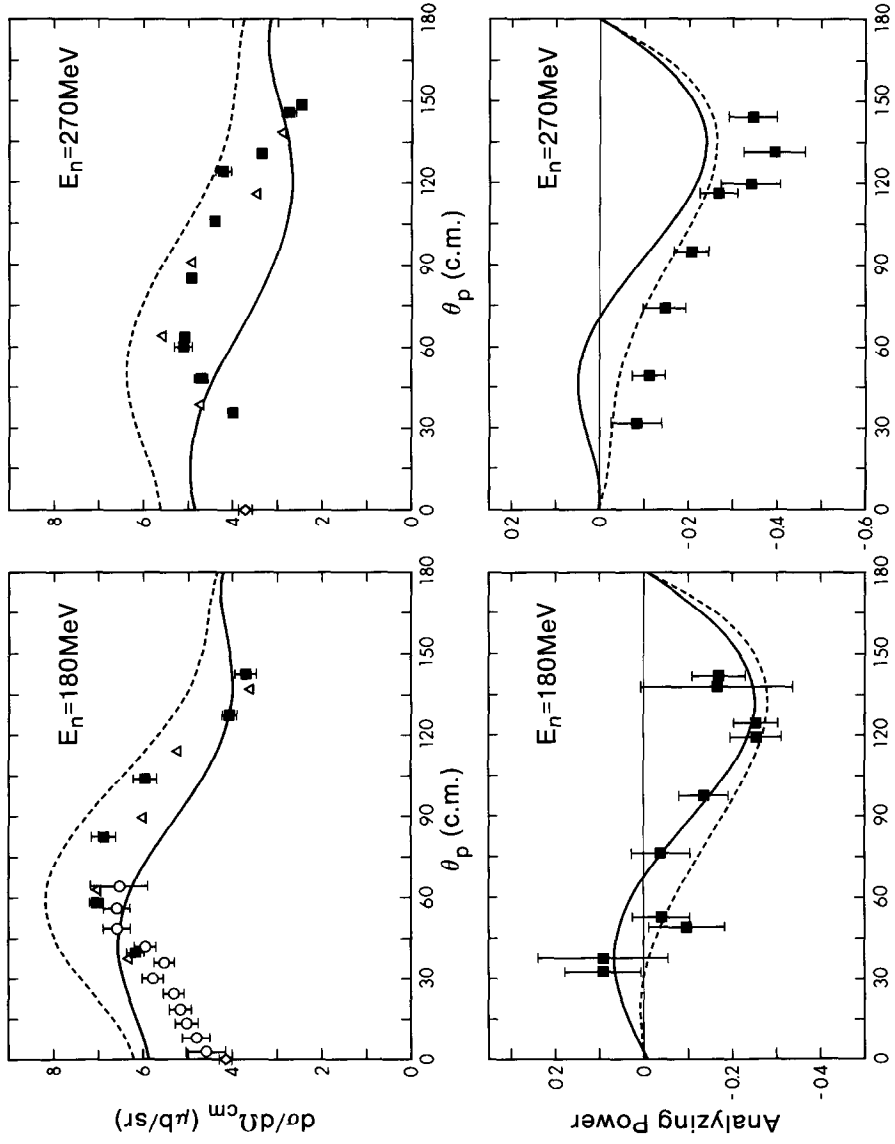

Fig. 8. Experimental data, see fig. 4, are compared to the result of a gauge invariant calculation (ref. [29])) for the nucleon current alone (dashed curve) and to that obtained by including meson exchange and isobar effects (solid curve).

potential used to calculate the $T = 1$ np wave functions has a one pion exchange part which takes into account the masses and coupling constants of both neutral and charged pions.

Recently a gauge invariant exchange current model has been constructed for the parameterized Paris potential and applied to the $np \rightarrow d\gamma$ reaction [29]). In addition to meson exchange operators the contributions of Δ-isobar excitations to the electromagnetic process are included. The predicted cross sections for the nucleon current alone (dashed curves) and that obtained by including meson exchange and

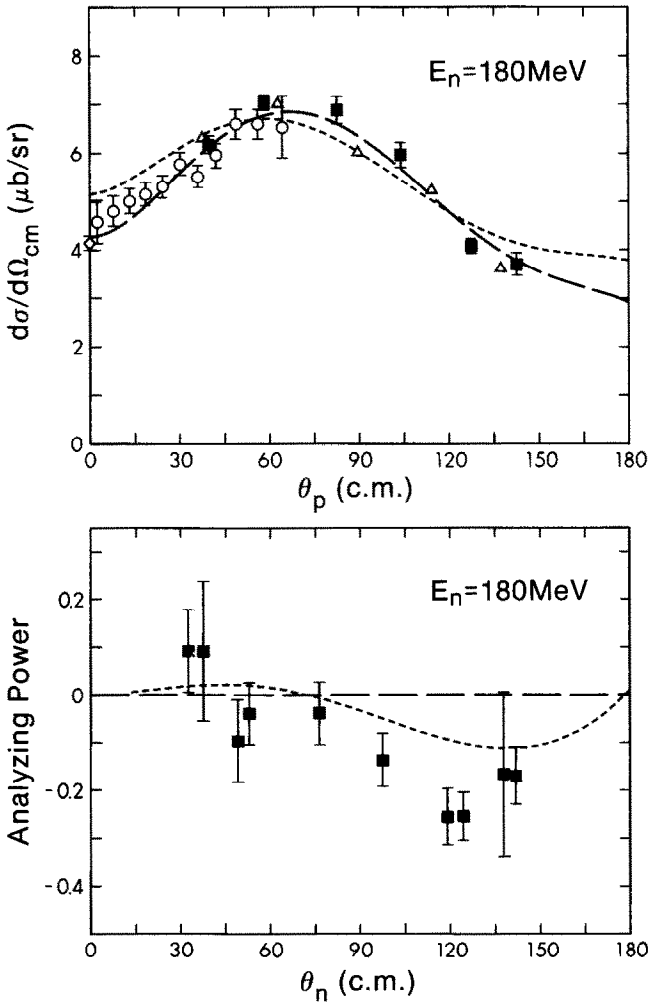

Fig. 9. The differential cross section and analyzing powers for $E_n = 180$ MeV are compared to the result of a calculation in which a series of scattering diagrams is summed (ref. [30])). The inclusion of np final state interactions (short dashed curve) is needed to obtain an analyzing power for the neutrons which is found to be zero for a plane wave calculation (long dashed curve).

isobar effects (solid curves) are compared to the data in fig. 8. The full calculation appears to have qualitatively the correct shape for the cross section but again it is too large at small angles, presumably due to the neglect of those relativistic corrections to charge and current operators discussed above. However, the comparison of the full calculation with the analyzing power data at $E_n = 270$ MeV again clearly demonstrates that the meson exchange and isobar contributions account for the negative asymmetries seen in the forward direction.

An alternative approach to photodisintegration has been to evaluate a series of elementary operators rather than using a potential [30]). This approach has certain advantages in that it is possible at each stage to insure gauge invariance by inclusion of the appropriate set of operators while relativistic effects are included to order $1/m^2$ in the expansion of the space components of the currents. On the other hand it is not possible to use a full off-shell treatment of the neutron–proton scattering which becomes important as all rescattering must be put in explicitly. While the np final state interactions do not greatly affect the differential cross section it is only when they are included in both S and P wave that one can reproduce the neutron analyzing powers which in plane wave are predicted to be zero, as shown in fig. 9. The inclusion of the final state interactions in S and P wave results, however, in an undesirable increase in the zero degree cross section; it is suggested that inclusion of higher partial waves might reproduce simultaneously this cross section and the measured analyzing powers [30]).

5. Conclusions

We have presented new data for the differential cross section and analyzing powers for the radiative capture on hydrogen of polarized neutrons at $E_n = 180$ and 270 MeV. The cross section data are in good agreement with other recent measurements of neutron radiative capture or using monoenergetic photon beams to disentegrate deuterons.

Comparison with various theoretical models in which the Paris potential is used shows that the differential cross section is sensitive to meson exchange and isobar current effects but that only when additional relativistic corrections are included does the agreement with the data become acceptable. The measured negative asymmetries at forward angles at $E_n = 270$ MeV are only reproduced in the potential model calculations when exchange current effects are added. One the other hand when the process is evaluated in terms of elementary operators the analyzing powers are very sensitive to details of the model and show the importance of including higher partial waves for the neutron proton rescattering.

References

1) W-Y.P. Hwang, Can. J. Phys. **62** (1984) 1072
2) W-Y.P. Hwang and G.E. Walker, Ann. of Phys. **159** (1984) 118

3) R.J. Hughes, A. Ziegler, H. Waffler and B. Ziegler, Nucl. Phys. **A267** (1976) 329
4) F. Partovi, Ann. of Phys. **27** (1964) 79
5) J.L. Friar, B.F. Gibson and G.L. Payne, Phys. Rev. **C30** (1984) 441
6) A. Cambi, B. Mosconi and P. Ricci, Phys. Rev. Lett. **18** (1982) 462; J. of Phys. **G10** (1984) L11
7) W. Jaus and W.S. Woolcock, Nucl. Phys. **A431** (1984) 669
8) E.A. Whalin, B.D. Schriefer and A.O. Hansen, Phys. Rev. **101** (1956) 377
9) J.C. Keck and A.Y. Tollestrap, Phys. Rev. **101** (1956) 360
10) Iu.A. Aleksandrov, N.B. Delone, L.I. Slovokhotov, G.A. Sokol and L.N. Shtarkov, Sov. Phys. JEPT **6(33)** (1958) 472
11) R. Kose, W. Paul and K. Stockhorst, Z. Phys. **202** (1967) 364
12) P. Dougan, V. Ramsay and W. Stiefler., Z. Phys. **A280** (1977) 341
13) G. Nicklas, J. Franz, E. Rossle and H. Schmitt, Phys. Lett. **141B** (1984) 170
14) J.M. Cameron, Can. J. Phys. **62** (1984) 1019
15) R. Abegg, J. Birchall, E. Cairns, H. Coombes, C.A. Davis, N.E. Davison, P.W. Green, L.G. Greeniaus, H.P. Gubler, W.P. Lee, W.J. McDonald, C.A. Miller, G.A. Moss, G.R. Plattner, P.R. Poffenberger, G. Roy, J. Soukup, J.P. Svenne, R. Tkachuk, W.T.H. van Oers, and Y.P. Zhang, Nucl. Instr. Meth. **A234** (1985) 11
16) J.M. Cameron, P. Kitching, W.J. McDonald, J. Pasos, J. Soukup, J. Thekkumthala, H.S. Wilson, R. Abegg, D.A. Hutcheon, C.A. Miller, A.W. Stetz, and I.J. van Heerden, Nucl. Phys. **A424** (1984) 549
17) J.M. Cameron, C.A. Davis, H. Fielding, P. Kitching, J. Soukup, J. Uegaki, J. Wesick, H.S. Wilson, R. Abegg, D.A. Hutcheon, C.A. Miller, A.W. Stetz, Y.M. Shin, N. Stevenson, and I.J. van Heerden, Phys. Lett. **137B** (1984) 315
18) R. Arndt, Interactive Dial-in Program SAID, private communication
19) H.O. Meyer, J.R. Hall, M. Hugi, H.J. Karwowski, R.E. Pollock, and P. Schwandt, Phys. Rev. Lett. **64** (1984) 1759
20) E. DeSanctis, G.P. Capitani, P. DiGiacomo, C. Guaraldo, Y. Lucherini, E. Polli, A.R. Reolon, R. Scrimaglio, M. Anghindfi, P. Corvisiero, G. Ricco, M. Sanzone and A. Zucchiatti, Phys. Rev. Lett. **54** (1985) 1639
21) D.O. Riska, Perspectives in Nucl. Phys. at Int. Energies, ed. S. Boffi *et al.* (World Science, 1984) p. 71
22) A.J.F. Siegert, Phys. Rev. **52** (1937) 787
23) T. Hamada and I.D. Johnston, Nucl. Phys. **34** (1962) 382
24) M.L. Rustgi, R. Vyas and O.J. Rustgi, Phys. Rev. **C29** (1984) 785
25) J.M. Greben and R.M. Woloshyn, J. of Phys. **G9** (1983) 643
26) M. Lacombe, B. Loiseau, J.M. Richard, R. Vinh Mau, J. Cote, P. Pires and R. de Tourreil, Phys. Rev. **C21** (1980) 861
27) R. de Tourreil and D.W.L. Sprung, Nucl. Phys. **A201** (1973) 193
28) K.E. Lassila, M.H. Hull, H.M. Ruppel, F.A. McDonald and G. Breit, Phys. Rev. **126** (1962) 881
29) A. Buchmann, W. Leidemann and H. Arenhovel, Nucl. Phys. **A443** (1985) 726
30) J.M. Laget, Can. J. Phys. **62** (1984) 1046; Nucl. Phys. **A312** (1978) 265